INFLUENCE OF THE DESIGN PARAMETERS ON THE INSTALLATION EFFECTS IN CORIOLIS FLOWMETERS

G. Bobovnik[1], J. Kutin[1], N. Mole[2], B. Štok[2], I. Bajsić[1]
University of Ljubljana, Faculty of Mechanical Engineering,
[1] Laboratory of Measurements in Process Engineering (LMPS),
[2] Laboratory for Numerical Modelling and Simulation (LNMS),
Aškerčeva 6, SI-1000 Ljubljana, Slovenia
gregor.bobovnik@fs.uni-lj.si

A computational study of the installation effects in Coriolis flowmeters positioned downstream of different flow disturbance elements (a single elbow, closely coupled double elbows out-of-plane and an orifice) is presented. The mass-flow sensitivities are estimated using the results of a fully three-dimensional, coupled and partitioned numerical model that accounts for the fluid-structure interactions. The results show that the mass-flow sensitivity can vary for different circumferential positions of the motion sensors in a straight-tube full-bore meter. Because of flow splitters and the averaging of the response of both measuring tubes, the installation effects are reduced in a twin-tube design.

Introduction

The available literature shows that there are relatively few systematic experimental or theoretical studies dealing with the installation effects in Coriolis flowmeters. The published experimental results [1-3] suggest that bent-tube meters could be, to a large extent, insensitive to inlet flow profiles, but also indicate that in some individual cases installation effects up to 0.5 % were detected. Unfortunately, the detection level of the installation effects in these experiments was considerably higher than the accuracy specifications of the latest-generation Coriolis flowmeters for measurements of the liquid flow rate (about 0.1 % of the measured flow rate); therefore, the installation effects are in need of further investigation.

The theoretical approaches that account for three-dimensional fluid flow effects represent an alternative to experimental investigations of the installation effects. We used CFD numerical modelling [4] and the weight-vector analysis [5] for some preliminary studies of the installation effects in straight-tube meters. Our findings showed that the integral effects of an order of magnitude of a tenth of a percent could be expected when a relatively short flowtube is positioned downstream of the single elbow.

The main objective of the present study is to identify the installation effects in a straight-tube full-bore meter and twin-tube meters with straight and U-tubes by means of numerical modelling for different upstream flow disturbances (see Fig. 1). The fully coupled, partitioned numerical model, already presented and validated in [6, 7], is used for an estimation of the installation effects.

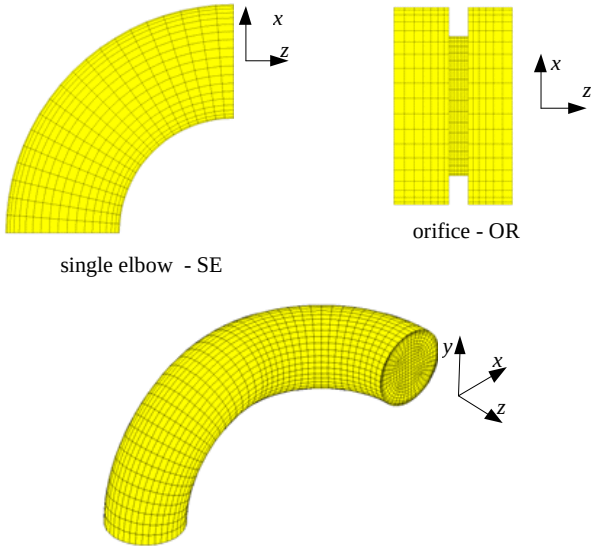

Figure 1. Flow disturbance elements (fluid domain)

Numerical model

The fluid-structure interaction in the measuring tube of the Coriolis flowmeter is simulated by linking the finite-volume code for the analysis of the turbulent fluid flow and the finite-element code for the analysis of the deformable shell structure. The numerical model used for the computer simulation is a partitioned one, using a conventional serial staggered procedure with a three-point fluid predictor for the fluid stress tensor and the additional inner iterations in each time step. The solution procedure is characterized by an alternative exchange of data between the two computational codes, where the data computed within one code provide the information to be used in the subsequent numerical step in the other code. A more detailed description of the simulation procedure, its validation and an analysis of the different coupling scenarios can be found in [6, 7].

This section presents the governing equations of the problem, the boundary and initial conditions, defines the computational domain, the material properties of the fluid and the structure, and the temporal and spatial discretization.

Fluid domain

Based on the assumption of a Newtonian, turbulent, isothermal and weakly compressible fluid flow with a density ρ_F, a fluid velocity vector $\boldsymbol{v}_F$ and a boundary velocity $\boldsymbol{v}_S$ of the fluid domain Ω_F, the conservation of mass and momentum principles can be written as

$$\frac{\partial}{\partial t}\int_{\Omega_F}\rho_F \mathrm{d}\Omega+\int_{\Gamma_F}\rho_F\left(\boldsymbol{v}_F-\boldsymbol{v}_S\right)\cdot\boldsymbol{n}\,\mathrm{d}\Gamma=0\,, \tag{1}$$

$$\frac{\partial}{\partial t}\int_{\Omega_F}\rho_F\boldsymbol{v}_F\,\mathrm{d}\Omega+\int_{\Gamma_F}\rho_F\boldsymbol{v}_F\left(\boldsymbol{v}_F-\boldsymbol{v}_S\right)\cdot\boldsymbol{n}\,\mathrm{d}\Gamma= \int_{\Gamma_F}\boldsymbol{\sigma}_F\cdot\boldsymbol{n}\,\mathrm{d}\Gamma+\int_{\Omega_F}\boldsymbol{f}_F\,\mathrm{d}\Omega\,, \tag{2}$$

where Γ_F is the boundary of the fluid domain, the vector $\boldsymbol{f}_F(x,t)$ stands for the volume forces acting inside the fluid domain Ω_F and $\boldsymbol{\sigma}_F(x,t)$ is the fluid stress tensor combining the viscous stresses and the pressure. The stresses due to turbulent motion are resolved by employing the standard k-ε turbulence model.

The numerical solution to the fluid problem was obtained by employing the commercial CFD code Star-CD v4.18. The unsteady terms are discretized in accordance with the implicit Euler scheme. The initial velocity field corresponds to the steady-state field of the fluid flow in the tube at rest. The fully developed velocity profile is set at the inlet boundary, while at the outlet the ambient pressure is imposed. The boundary velocities are only prescribed for the surface of the measuring tube section, according to the results of the solid domain analysis. A moving grid simulation is performed to capture the motion according to the results of the solid domain analysis. The FVs' boundary velocities are calculated by obeying the so-called space-conservation law.

The flow domain is schematically presented in Fig. 2 for a twin U-tube meter positioned downstream of the double elbow disturbance. It consists of the flow disturbance section, the inlet section (consisting of a straight tube run and, in the case of the twin-tube meters, also of the flow splitter), the measuring tube section and the outlet section. The three different disturbance elements shown in Fig.1 are modelled: the single elbow (SE), the closely coupled double elbows out-of-plane (DE) and the orifice-like constriction (OR). In all the presented simulations the flow disturbance elements are positioned $5D_{in}$ upstream of the single measuring tube or the flow splitter in the twin-tube design (where D_{in} is the inner diameter of the inlet tube). The single elbow and the downstream elbow of the double elbows out-of-plane configuration are positioned in the x-z plane. In the reference case, used to model the fully developed fluid flow conditions in the measuring tube, only the straight inlet section of length $10D_{in}$ was assumed to be upstream of the measuring tube.

All the elbows have a centreline curvature radius of $1.5D_{in}$, and the inner diameter and the thickness of the orifice equal $D_{in}/\sqrt{2}$ and $0.1D_{in}$, respectively. The inner diameter of the measuring tube walls for all the modelled cases equals $D=20$ mm. For the straight-tube full-bore meter model $D_{in}=D$ and in case of the twin-tube meters model $D_{in}=50$ mm.

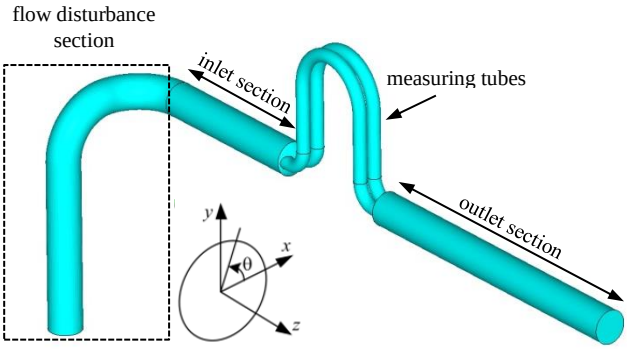

Figure 2. Scheme of the fluid computational domain (twin U-tube meter positioned downstream of the double elbows out-of-plane)

All the simulations were performed for a water-like fluid with a density of 1000 kg/m^3 and a viscosity of 0.001 Pa·s. The mass flow rate of the fluid in the straight-tube full-bore meter model was equal to $q_m=1.57$ kg/s and was twice as large in the twin-tube meter simulations, with the purpose being to obtain comparable flow velocities in the measuring tubes for all the simulated cases.

Solid domain

The three-dimensional spatial distribution and time evolution of the tube's dynamic response are governed by the conservation of momentum principles. The associated equation of motion can be derived using Hamilton's variational principle, which can be written as

$$\int_{t_1}^{t_2}\delta\left(E_p-E_k\right)\mathrm{d}t=0\,, \tag{3}$$

where E_p and E_k are, respectively, the total potential energy and the total kinetic energy of the moving solid structure under consideration. The total potential energy E_p is the sum of the strain energy corresponding to the actual deformation of the tube, and the load's potential corresponding to the actually applied conservative external forces. Considering the nature of the investigated case, the surface tractions $\mathbf{p}_S$ acting on the moving tube boundary through the respective displacement field $\mathbf{u}_S$, and the concentrated force $\mathbf{F}$ at the points P_i, where the forced vibration is generated, are taken into account. These loads yield the following integral expression for the total potential energy

$$E_p=\tfrac{1}{2}\int_{\Omega_S}\boldsymbol{\sigma}_S:\boldsymbol{\varepsilon}_S\,\mathrm{d}\Omega-\int_{\Gamma_S}\mathbf{p}_S.\mathbf{u}_S\,\mathrm{d}\Gamma-\sum_i\mathbf{F}.\mathbf{r}_{P_i}\,. \tag{4}$$

In the above equation, Ω_S is the tube domain and Γ_S is its boundary. $\boldsymbol{\varepsilon}_S$ and $\boldsymbol{\sigma}_S$ are, respectively, the strain and the stress tensors in the tube, and $\mathbf{r}_{P_i}$ is the position vector of the point P_i where the force $\boldsymbol{F}$ is applied. The total kinetic energy E_k of the tube can be written as

$$E_k = \tfrac{1}{2} \int_{\Omega_S} \rho_S \, (\boldsymbol{v}_S \cdot \boldsymbol{v}_S) \, \mathrm{d}\Omega \,, \qquad (5)$$

where ρ_S is the density of the tube material and $\boldsymbol{v}_S$ is the tube's velocity field.

The numerical analysis of the vibrating measuring tube(s) (modelled as a deformable shell structure with isotropic, linear elastic, material properties) and the attachments (modelled as solids and discrete mass elements) was realised using the commercial code Abaqus 6.10, which solves a dynamics problem in accordance with the finite-element method. The Newmark formulae are used for the implicit displacement and the integration of velocity over time.

The numerical domain for the structural dynamic analysis consists only of the vibrating measuring tube(s) clamped at both ends and additional elements (masses) attached to it. Three different designs of the Coriolis flowmeters were considered: a straight-tube full-bore meter, a twin straight-tube meter and a twin U-tube meter. The details of the considered geometries are shown in Fig. 3 (the fluid domain – in blue – is included for better representation); the discrete mass elements representing the exciters (at the middle) and the sensors (positioned symmetrically with respect to the centre of the measuring tube's length) are represented by yellow points.

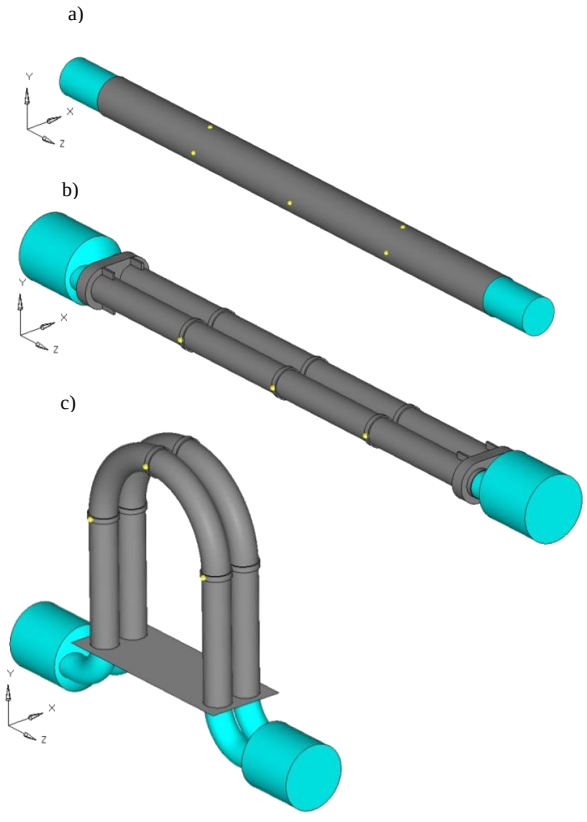

Figure 3. Flowmeters designs - a) straight-tube full-bore meter, b) twin straight-tube meter and c) twin U-tube meter

The effective length of the measuring tubes (L_m) was equal to 15D or 20D and its thickness (s) to 1 mm (if not stated otherwise). The sensor masses are assumed to be equal to 1 g and the rings (representing the local reinforcement caused by the different means of attaching the exciter or the sensors to the measuring tube) are assumed to be 1 mm thick and 4 mm wide. The measuring tube and the other attachments are assumed to be made of titanium with a density of 4510 kg/m^3, a Young's modulus of 102.7 GPa and a Poisson's ratio of 0.34.

The initial velocity, corresponding to the first natural lateral vibration mode, is prescribed as the initial condition. The initial mechanical state of the measuring tube is assumed to be unstressed and unstrained. The imposed boundary conditions are the clamped ends of the measuring tube(s), the time-varying pressure load of the fluid on the inner side obtained with the fluid analysis, and the time-varying excitation forces due to the forced vibration on the outer side of the measuring tube. The excitation forces are applied to the middle of the measuring tube(s) and the excitation is, in all cases, modelled in the x-direction. The measuring tubes in the twin-tube meters are driven to vibrate in anti-phase to each other.

Temporal and spatial discretization

The measuring tube is discretized using the structured mesh of shell finite elements, which divide the tube's circumference into 40 segments and have an approximate axial length of about 4 mm (refined at the attachments' positions). The surface of the fluid in the measuring tube has the same discretization as in the solid model. The cross-section of the tube is discretized using 441 cells. The time step of the simulation is set to 1/70 of the oscillation period of the measuring tube. All the simulation results presented in the text were conducted for 3000 time steps.

The repeatability (estimated scatter) of the calculated installation effects is lower than 0.02 % for all the simulated cases. For the single straight-tube full-bore meter model ($L_m = 15D$) it was proven that either refining the axial discretization or reducing the time step size by a factor of 2 has only a minor influence on the estimated installation effects; the installation effects differed by less than 0.01 % compared to the reference case.

Estimation of the installation effect

The mass-flow sensitivity of the Coriolis flowmeter can be defined by the ratio between the time difference ($\Delta t_S = \Delta\phi / 2\pi f_0$) exhibited by the periodic responses of the motion sensors and the mass flow rate q_m through the measuring tube, $K_{\Delta t} = \Delta t_S / q_m$. The frequency ($f_0$) and the phase ϕ at f_0 for each individual response with a length of 10 oscillation periods were obtained using a discrete Fourier transform algorithm and the phase difference $\Delta\phi$ was calculated as the difference between the phase values of the sensors' responses. The estimation of the installation effect is given by the relative change of the mass-flow sensitivity ε_K obtained for the disturbed flow conditions with respect to the fully developed flow conditions in the measuring tube.

Results

Straight-tube full-bore meter

The installation effects (ε_K) for the straight measuring tube of length 15D (the exciters and the sensors were considered massless) positioned downstream of the different flow disturbance elements are shown in Fig. 4 for different circumferential positions of the sensing points (see Fig. 2 for the definition of θ).

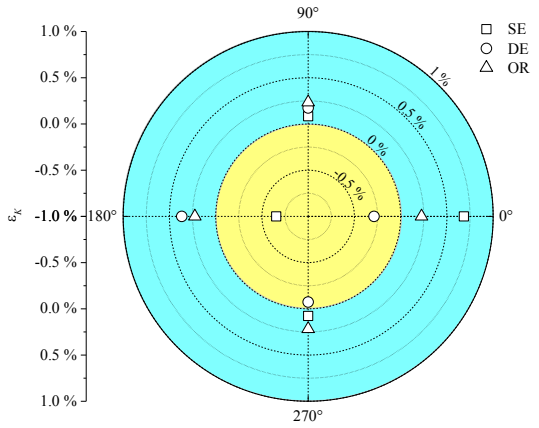

Figure 4. Variation of ε_K for the measuring tube with a length of 15D downstream of a) SE, b) DE, c) OR

The single or the double elbows cause the measuring tube not to respond uniformly around the entire circumference. In the case of the single elbow configuration, the sensitivity of the flowmeter, when observed at sensing points positioned in the plane perpendicular to the elbow at θ = 90° and 270°, remains almost unaltered (lower than 0.1 %). Much larger effects are found in the elbow's plane (at θ = 0° and 180°) in which the asymmetrical distortion of the velocity profile occurs (up to ±0.7 %).

The circumferential installation effect variations seem very complex when the flowmeter is positioned downstream of the double elbows. However, the estimated errors are lower than in the case of the single elbow, which is presumably due to the smaller asymmetry of the distorted axial velocity profile. The orifice produces, in contrast to the previous two cases, an almost constant relative change of sensitivity for the different sensors' circumferential positions. This is expected due to the axi-symmetric velocity profile distortion downstream of the orifice.

In Fig. 5 we compared the installation effects for different measuring tubes. The reference measuring tube (L_m = 15D, s = 1 mm) was compared to a longer measuring tube (L_m = 20D), a thicker measuring tube (s = 1.5 mm) and a measuring tube with rings placed at the exciters' and sensors' positions – similar to the twin straight-tube meter in Fig. 3b.

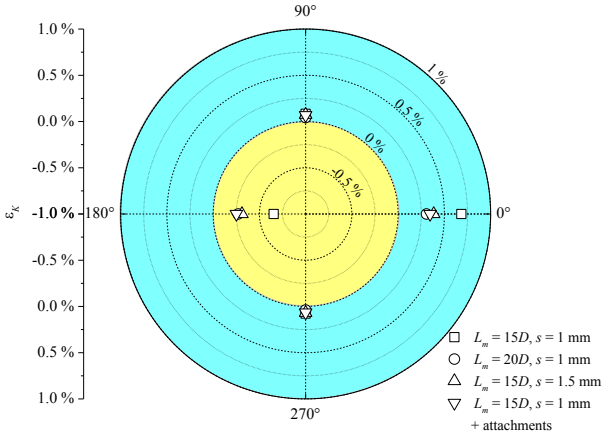

Figure 5. Variation of ε_K for different measuring tubes downstream of SE

The installation effect has the same trend along the circumference for all four cases; however, the amplitude at θ = 0° and 90° is reduced by approximately a factor of 2 for all cases, compared to the reference case. The response of the longer measuring tube resembles more a "slender beam" behaviour, which means smaller shear deformations across the cross-section. Similarly, the thicker tube also responds more uniformly along the circumference due to the increased circumferential stiffness of the measuring tube. Local reinforcements caused by attaching the rings demonstrate a similar effect to the increased wall thickness of the measuring tube.

The difference between the fluid forces acting on the downstream and upstream halves of the measuring tube, which could be related to the measuring effect, was also observed at different circumferential intervals. It was found that the amplitudes of such Coriolis-like fluid forces in the cross-section of the measuring tube depend proportionally on the magnitudes of the local axial fluid velocities. This further explains the relative change (increase or decrease) of the mass-flow sensitivity along the circumference in the case of non-symmetrically disturbed flows and why they are more profound in the measuring tubes with a smaller circumferential stiffness.

Twin-tube meters

The installation effects for the twin-tube meters were estimated for the single elbow and the double elbow flow disturbances, which cause the downstream non-symmetrical velocity profile alteration. The simulations were performed for the two variants of the twin straight-tube meter (the first is presented in Fig. 3b and the second is identical to the first, except that it does not include the attachments – rings and added masses of the exciters and sensors) and the twin U-tube meter shown in Fig. 3c. The results of the estimated installation effects are presented in Table 1. The integral value of the installation effect considering the response from all four sensors (two on each measuring tube) as well as the individual values of both measuring tubes (viewed in the x-direction the measuring tube 1 lies behind the measuring tube 2) are indicated.

Table 1. Values of ε_K for the twin-tube meters positioned upstream of SE and DE

	SE	DE
twin straight-tube meter (Fig. 3b)	**-0.01 %**	**-0.15 %**
measuring tube 1	-0.01 %	-0.12 %
measuring tube 2	-0.01 %	-0.19 %
twin straight-tube meter (Fig. 3b without the attachments)	**-0.09 %**	**-0.22 %**
measuring tube 1	-0.09 %	-0.14 %
measuring tube 2	-0.09 %	-0.29 %
twin U-tube meter (Fig. 3c)	**0.00 %**	**0.01 %**
measuring tube 1	0.08 %	0.05 %
measuring tube 2	-0.08 %	-0.04 %

It is clear that the estimated integral installation effects are very small (below 0.10 %) in almost all cases; with the exception of the twin straight-tube meter positioned downstream of the double elbow, where the estimated installation effect equals −0.15 % (−0.22 % for the model without the attachments). Observing each measuring tube individually we see that in all cases (except for the twin straight-tube meter downstream of the single elbow) the estimated installation effect is slightly higher/lower than its integral value. The largest variation is seen in the U-tube meter downstream of the double elbow, where the values of ε_K differ by ±0.08 % from the integral value. The integral value of the installation effect in this case is equal to zero, because the mass-flow sensitivity is determined by taking into account the "averaged" motion of both measuring tubes. A similar improvement could also be achieved in the straight-tube full-bore meter if four motion sensors positioned on opposite sides of the circumference were to be used for the estimation of the mass-flow sensitivity; it was checked to see that the installation effect could be reduced below 0.1 % in that manner for the 15*D* measuring tube positioned downstream of the single elbow.

Comparing the individual installation effects of both measuring tubes of the twin straight-tube meter without the attachments with the values obtained for the 20*D* straight-tube full-bore meter in Fig. 4, it is obvious that their magnitudes are different. This is most probably related to the presence of the flow splitters, which additionally modify the velocity profile in the measuring tubes. It is very likely that each flow splitter design has a different effect on the installation effects in Coriolis flowmeters. The results in Table 1 also show that the other geometry parameters (shape, stiffness, added masses, etc.) influence the performance of the twin-tube Coriolis flowmeters.

Conclusions

A study of the installation effects in different Coriolis flowmeters using a fully coupled numerical model is presented. The installation effects were observed for flowmeters positioned downstream of a single elbow, a closely coupled double elbows out-of-plane and an orifice-like constriction.

The obtained results for a straight-tube full-bore meter show that the installation effects vary along the circumference of the tube, but can be reduced by increasing the length or the circumferential stiffness of the tube. Such circumferential variations are related to the local axial fluid velocities in the cross-section of the measuring tube. The highest installation effects of the order of several tenths of a percent were therefore predicted downstream of the single elbow, with sensors positioned in the plane of the elbow.

On the other hand, the common twin-tube meters show a significantly smaller susceptibility to the installation effects. Taking into account the motion of both measuring tubes, the presence of the flow splitters and the slender measuring tubes with local reinforcements (caused by different methods of sensor or exciter fixations) all contribute to a minimization of the installation effects.

References

[1] T. Patten, G. Pawlas, "The effect of swirl on Coriolis mass flowmeters" in proceedings of North Sea Flow Measurement Workshop; 1995; Lillehammer, Norway.

[2] R. Cheesewright, C. Clark, D. Bisset, "The identification of external factors which influence the calibration of Coriolis massflow meters". Flow Measurement and Instrumentation, Vol. 11, pp. 1-10, 2000.

[3] T.A. Grimley, "Installation effects testing of Coriolis flow meters with natural gas", In: Proceedings of the 5th International Symposium on Fluid Flow Measurement, 2002, Arlington, Virginia.

[4] G. Bobovnik, J. Kutin, I. Bajsić, "The effect of flow conditions on the sensitivity of the Coriolis flowmeter", Flow Measurement and Instrumentation ; Vol. 15, pp. 69-76, 2004.

[5] J. Kutin, G. Bobovnik, J. Hemp, I. Bajsić, "Velocity profile effects in Coriolis mass flowmeters: recent findings and open questions", Flow Measurement and Instrumentation, Vol. 17, pp. 349-358, 2006.

[6] G. Bobovnik, N. Mole, J. Kutin, B. Štok, I. Bajsić, "Coupled finite-volume/finite-element modelling of the straight-tube Coriolis flowmeter", Journal of Fluids and Structures, Vol. 20, pp. 785-800, 2005.

[7] N. Mole, G. Bobovnik, J. Kutin, B. Štok, I. Bajsić, "An improved three-dimensional coupled fluid-structure model for Coriolis flowmeters". Journal of Fluids and Structures, Vol. 24, pp. 559-575, 2008.